

Conservation Issues for RANS-Based Rotor Aeroelastic Simulations

Marilyn J. Smith
Daniel Guggenheim School of Aerospace Engineering
Georgia Institute of Technology
Atlanta, GA 30332-0150, USA

Abstract

The numerical errors introduced during aeroelastic (CFD–CSD) rotor simulations relative to conservation of the structural and fluid dynamics equations of motion are discussed and quantified. The preservation of work during the transfer of data loads and deflections between the fluid/structure interface is discussed for lifting-line and lifting-surface beam models, using structured and unstructured CFD solvers. It is shown that interpolation methods with C^0 and higher are required to preserve the work for both spatial and temporal interfaces. A method to obtain the CSD airstation distribution with the minimal data transfer error for a given grid is discussed. Unstructured CFD methods appear to be more sensitive to the level of continuity (consistency) of the methods than structured solvers.

Nomenclature

$d\mathbf{r}$	Displacement vector, m
f	Function
\mathbf{F}	Force vector, N
\mathbf{F}	Combined force and moment vector
$[\mathbf{G}]$	Interpolation matrix
$[\mathbf{H}]$	Shape function
$[\mathbf{I}]$	Identity matrix
ℓ	Beam length, m
\mathbf{M}	Moment vector, N-m
N	Maximum number of nodes
\mathcal{O}	Order or approximation
\mathbf{Q}	Nodal loads
r	Position vector, m or shape parameter
\mathcal{R}	Multidimensional space
S	Surface or area, m^2
S	Spline
t	Time, s
\mathbf{x}	Variable value vector
V	Velocity vector, m/s
W	Work, N-m
x, y, z	Cartesian components of position, m
α	Rotation angle vector
β	Coefficients for 2–D splines
Δ	Difference
γ	Coefficients for 2–D splines
ϵ	Error
Ω	Azimuth, degrees
<i>Subscript and Superscript</i>	
i, j	Variable number
T	Matrix transpose

Ω	Azimuthal Location
-1	Matrix inverse
<i>Abbreviations</i>	
<i>CFD</i>	Computational Fluid Dynamics
<i>CSD</i>	Computational Structural Dynamics
<i>MQ</i>	Multiquadric-Biharmonic Method
<i>TPS</i>	Thin Plate Spline

Introduction

The development of efficient numerical techniques to accurately simulate rotor airloads, vibration characteristics and noise signatures has been a major focus of research for the past twenty to thirty years within the rotorcraft community. The rotor flow field is a complex interaction of nonlinear unsteady aerodynamics and structural dynamics, which must be trimmed for level flight or controlled during a maneuver. The aerodynamics includes the incompressible Mach region, where it may encounter high angle of attack/separated flow, as well as high-speed flight in the transonic and low supersonic Mach region. In addition, for low-speed forward or hover flight conditions, the wake system does not propagate rapidly downstream, but remains in the near field of the rotor, adding vortex interactions that must be modeled. The dynamics of the rotor include coupled flapping, pitching, and lead/lag motion, along with nonlinear elastic blade deformations that result from the unsteady aerodynamics loading. Thus an accurate prediction of the rotor behavior is an inherent aeroelastic

problem that relies on the accurate prediction of all of these components.

While the external dynamics of the problem must be modeled accurately, improvement of aeroelastic methods has centered on the independent development of accurate, efficient resolution techniques of the fluid and structural dynamics equations of motion. It is well-known that the equations of motion that describe the fluid flow field and elastic structure are very different, resulting in computational techniques and grid requirements that are significantly different. Two classes of solutions for rotorcraft applications have evolved from these requirements. The first, and earliest, class of solution methodologies has resulted in a set of computational techniques known as comprehensive codes, which are characterized by the utilization of finite-element structural methods combined with lower-order aerodynamics, such as lifting-line, dynamic inflow, and prescribed or free wake models. Most of the earlier versions of these codes operated in the frequency domain, although the recent trend has been toward time-domain-based algorithms. The attraction of these comprehensive codes is their ability to obtain aeroelastic simulations very rapidly for design and operations analysis, but it comes at the price of reduced aerodynamic fidelity resulting in less accurate prediction of the rotor behavior during some flight conditions. Among the most popular of these codes are DYMORE [1, 2], RCAS [3], CAMRAD II [4], UMARC [5], and HOST [6]. A detailed discussion of the current capabilities of a number of these comprehensive codes can be found in Kunz [7].

As computational capabilities have improved, and as researchers begin to develop advanced blade concepts, the need for improved aerodynamic modeling in these simulations has resulted in the development of more accurate, though much more costly, computational techniques. In particular, for the last decade, numerical research has focused on techniques to harness the capabilities of the nonlinear, finite-element, multi-body modules of these comprehensive or computational structural dynamics codes (CSD), as well as the higher aerodynamic resolution capabilities found in computational fluid dynamics (CFD) codes that resolve the Reynolds-Averaged Navier-Stokes (RANS) equations. This class of simulations has become known in the rotorcraft community as CFD-CSD coupling. The history of the development of CFD-CSD coupling methods can be found in Datta *et al.* [8], along with some significant early efforts in the 1990's [9, 10], that were not included in the review. Some notable recent work extending the CFD-CSD techniques [11] – [15] are also recommended to obtain a synopsis of the current state-of-

the-art.

While some thought has been given towards the development of a new *fully-coupled* numerical simulation, where the entire set of fluid and structural mechanics equations are resolved simultaneously, most aeroelastic development has concentrated on utilizing existing (legacy) CFD and CSD codes, giving rise to *tightly-coupled* and *loosely-coupled* simulations. Within this work, tight coupling refers to the situation where data are exchanged between the CFD and CSD codes at each time step (or small subset of CFD timesteps) during a revolution of the rotor, while a loosely-coupled analysis exchanges data for an entire revolution of the rotor. While these CFD-CSD methods have improved the ability of the rotorcraft community to capture major nonlinear phenomena, they have additional numerical complexities that must be optimized to reduce numerical errors.

Any numerical simulation technique is inherently susceptible to errors due to a variety of sources. For rotorcraft simulations, these errors can run the gamut from engineering simplification assumptions, such as turbulence models, lack of geometric conservation laws, and geometrically inexact representation of the rotor blade, to numerical truncation errors associated to spatial and temporal algorithms to represent the governing equations, to round-off errors from floating point operations. These are all well recognized sources of error within each discipline, and the methods to mitigate them are extensively documented and will not be pursued here. However, when one considers the numerical simulation of a flexible rotor via loose or tight coupling, a new set of errors arises that is associated with the need to exchange data between two disparate solution techniques and grids. Consider a typical delta airloads coupling technique (for example, Fig. 1) utilized by many CFD-CSD methodologies. Within the CFD analysis, the pressure variable at each node on the rotor surface blade is computed. However, the aerodynamic load or force is needed by the CSD code, requiring the integration of these pressures over the area of the blade covered by the CFD grid. If the CFD and CSD surface grids are not coincident, then a transfer of loads between the two grids is necessary. Conversely, the blade deflections are computed at the CSD nodes, which then must be transferred to the CFD grid. Since interpolations and possibly extrapolations are needed, small differences arise whenever the data is transferred. While this error may be small at one calculation, it must be noted that this information is typically transferred at each one degree or less azimuth, resulting in 360 or more exchanges per revolution.

Most current CFD-CSD coupling methods are based on a lifting-line interpolation. That is, the

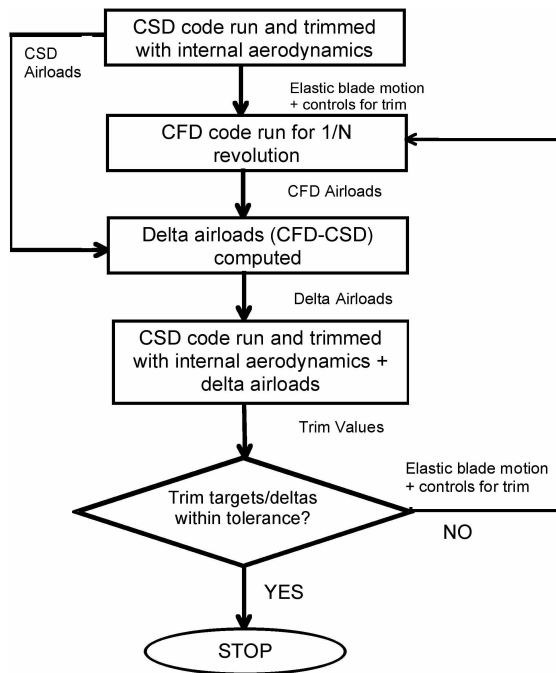


Figure 1: Example of CFD-CSD loose coupling, where N =number of rotor blades.

blade is treated as a beam with bending and torsion only along the radial axis, with the airfoils (chord-wise axis) remaining rigid. This allows integration of forces and moments about a blade strip, with the data transfer at a given chord location (usually quarter-chord), as illustrated in Fig. 2a. Comparison of different CFD-CSD coupling results has raised the question of the importance of interpolation/extrapolation errors in this data transfer. One technique that has been utilized to mitigate these interpolation errors in light of these questions, is to set the structural airstations to be coincident with the midpoint of the CFD spanwise strips (Fig. 2b). This will aid in the minimization of errors across the fluid/structure interface, but with the advent of unstructured methods for CFD-CSD coupling, the naturally occurring integration strips are no longer straightforward, as shown in Fig. 2c. In addition, if advanced blade designs incorporating aeroelastic-tailoring techniques that modify the local airfoil camber are to be modeled, then the simplified lifting-line data transmission will need to be expanded to a lifting-surface model.

Methods to mitigate these data errors have been studied and published for fixed-wing applications, of which a representative subset can be found in Refs. [16] – [21]. These prior studies clearly indicate that the transfer of data in aeroelastic simulations is not a triviality that can be ignored. They provide a basis from which this work addresses the topic of data transfer across the fluid/structure interface specifi-

cally for CFD-CSD coupling of rotors.

This paper will first address the concept of using variational quantities as a metric to assess the fluid/structure interface compared to a metric based upon vector quantities. Next, studies involving legacy CFD and CSD using current coupling practices illustrate the impact of the data transfer across the fluid/structure interface for beam and surface representations of rotor blades, and from these results best practices are extracted.

Variational Quantity Analysis

The analysis of the quality of CFD simulations applies the branch of analytical mechanics known as vectorial mechanics, where vector properties (forces, moments, momentum) are the foci of correlation. These quantities provide an instantaneous snapshot of the flow field variables at each time step and work well when correlating with theoretical and experimental field data. By definition, however, aeroelasticity involves the change of these vectors over time and/or space. Within the field of analytical mechanics, the assessment of an aeroelastic simulation can be extrapolated to the branch known as variational principles (energy principles). These approaches scrutinize the system changes in temporal or spatial dimensions through the use of work and energy parameters. Thus, the balance of the forces and moments is necessary, but not sufficient; the equivalence of the total work between the CFD and CSD methods is also necessary.

For example, the work can provide a more meaningful assessment of how well the data manipulation across the disparate aerodynamic and structural grids has been accomplished as it includes both the forcing function (aerodynamic load) and its response (blade deflection). To apply this, first consider the work on a particle that, under the influence of an external force \mathbf{F} moves from point a to b

$$W|_a^b = \int_a^b \mathbf{F} \cdot d\mathbf{r} \quad (1)$$

For the aeroelastic problems of interest in this work, the force in eqn. 1 consists of the aerodynamic forces on a rotor blade and the distance is the elastic displacement of the rotor blade. In addition, work done by the moments \mathbf{M} applied with the rotation vector, $\boldsymbol{\alpha}$, should also be considered, resulting in the total work at each azimuthal location, Ω ,

$$W^\Omega = \int_S (\mathcal{F} \cdot \mathbf{r}) dS = \int_s (\mathbf{F} \cdot \mathbf{r} + \mathbf{M} \cdot \boldsymbol{\alpha}) ds \quad (2)$$

when the pressure and viscous forces, together denoted as \mathcal{F} are integrated over the blade surface S , or

the forces \mathbf{F} and moments \mathbf{M} per unit span are integrated over a reference radial axis, s . Since the rotor blade is discretized as part of the numerical analysis, the integral equation can be replaced by a summation. For example, the integral over the reference axis would become

$$W^\Omega = \sum_{i=1}^N (\mathbf{F}_i \cdot \mathbf{r}_i + \mathbf{M}_i \cdot \boldsymbol{\alpha}_i) \quad (3)$$

where the i subscripts indicate the discrete counterparts to the continuous functions. It is assumed that the rotor surface is not changing shape at each instant when data are transferred between the CFD and CSD modules, so the errors incurred during the data transfer across the fluid/structure common interface can be analyzed via the equivalency of work, that is

$$W^{CFD} = W^{CSD} \quad (4)$$

Thus for a rotor blade at the same azimuthal location, the work computed from disparate CFD and CSD rotor models should be equivalent. In other words, the fluid/structure interface will contribute no errors to the system's conservation of work (or energy) if the difference in the work for each method, ϵ , is zero:

$$W^{CFD} - W^{CSD} = \epsilon = 0 \quad (5)$$

When ϵ is non-zero, it can be utilized as a measure of the CFD-CSD grid interpolation error that detracts from the conservation of the system.

Consider next the transfer of discrete data, $\{\hat{\mathbf{f}}\}$, (for example, forces, loads or deflections) across the fluid/structure interface, which can be expressed as

$$\{\hat{\mathbf{f}}\}^{CFD} = [\mathbf{G}]\{\hat{\mathbf{f}}\}^{CSD} \quad (6)$$

where $[\mathbf{G}]$ is the transformation or interpolation method. Each element of the $\{\hat{\mathbf{f}}\}$ array can be expressed as

$$\hat{f}_i^{CFD} = \sum_{j=1}^{N^{CSD}} G_{ij} \hat{f}_j^{CSD} \quad (7)$$

The work at the fluid/structure interface can be computed using the discrete CFD grid locations

$$W^{CFD} = \sum_{i=1}^{N^{CFD}} \mathcal{F}_i \hat{\mathbf{r}}_i \quad (8)$$

while the work computed on the rotor blade using the discrete CSD grid locations can be expressed as

$$W^{CSD} = \sum_{j=1}^{N^{CSD}} \mathcal{F}_j \hat{\mathbf{r}}_j \quad (9)$$

where \mathcal{F} represents the integration of the pressure loads and viscous forces and the i and j subscripts denote distinct locations used by the CFD and CSD methods, respectively, to exchange data. If displacement, $\hat{\mathbf{r}}_i$, is used as the data, \hat{f} in the transformation relation of eqn. 7, and it is substituted into eqn. 6, then the work can be expressed as

$$W^{CFD} = \sum_{j=1}^{N^{CSD}} \left(\sum_{i=1}^{N^{CFD}} \mathcal{F}_i G_{ij} \right) \hat{\mathbf{r}}_j \quad (10)$$

and finally it can be readily seen that in comparison with eqn. 9 that

$$\mathcal{F}_j = \sum_{i=1}^{N^{CFD}} \mathcal{F}_i G_{ij} \quad (11)$$

It has been noted [16] that energy across the fluid/structure interface is conserved if the virtual form of eqn. 4 is achieved.

This discrete force, \mathcal{F}_i is obtained at the CFD grid node or cell center, depending on the computational method. If all of the CFD force locations are coincident with the structural airstations, then the discrete deflection values, r_i and r_j , are coincident and are directly extracted from the CSD methodology. Since $[\mathbf{G}] = [\mathbf{I}]$, it is easy to confirm that the balance of force and work is satisfied, and that the conservation is limited only by the intrinsic assumptions of the individual aerodynamic and structural mechanical modules.

However, if the grid nodes and airstations are not co-located, then $[\mathbf{G}]$ is no longer the identity matrix and errors may arise if the interpolation method is not consistent. Most of the CSD methods utilized for CFD-CSD rotor coupling are based on finite element techniques. The natural interpolation functions would therefore be those based on finite element interpolation methods. Indeed, once the loads are interpolated to the CSD airstations, they should be transferred to the modes of the structural node using the shape function of the local finite element to ensure proper evaluation of the work done by these forces. This is illustrated by a simple beam undergoing bending

$$\begin{aligned} W &= \int_0^\ell F(x)z(x)dx \\ &= \hat{z}^T \int_0^\ell H^T(x)F(x)dx \\ &= \hat{z}^T \sum_{i=1}^{nodes} H(x_i)F_i \\ &= \hat{z}^T \mathbf{Q} \end{aligned} \quad (12)$$

where $H(x)$ stores the shape functions of the beam element, and where \mathbf{q} are the nodal loads applied to the structural model. When nodal loads are computed using eqn. 12, the work done by the aerodynamic forces is properly transferred to the structural model. Poor quality interpolations can thus be exacerbated once the consistent loads are applied to the structure via eqn. 12. Various techniques to minimize the interpolation errors via the formulation of appropriate interpolation methods, $[\mathbf{G}]$ have been developed (Refs. [16] - [21]) for application to fixed-wing aeroelastic problems.

The aeroelastic analysis of a rotor in flight involves not only the interpolation of the rotor blade surface grids but also the temporal integration of the system. To examine this aspect of the problem, consider again the definition of work on a particle, eqn. 1, where the displacement of the particle is now recast in a parametric form with respect to time, $\mathbf{r}(t)$, so that the equation for work becomes

$$W|_{t_1}^{t_2} = \int_{t_1}^{t_2} \mathbf{F} \cdot \frac{d\mathbf{r}}{dt} dt = \int_{t_1}^{t_2} \mathbf{F} \cdot \mathbf{V} dt \quad (13)$$

This equation can be manipulated to examine temporal interpolation errors associated with the transfer of motion data applied to the rotor blade as it rotates about the hub. Just as the spatial scales needed to resolve the CFD and CSD governing equations are different, so are the temporal integration scales. CFD-CSD rotor simulations are typically accomplished using 0.05° to 1° azimuthal increments by the CFD code, while the CSD code is stable and accurate using larger (5° to 15°) azimuthal increments, depending on the flight conditions under evaluation. Since the CSD simulations are often far less expensive computationally than their CFD counterparts, one solution to the disparate time steps is to use the smaller CFD time step within the CSD simulation, eliminating the need for interpolations. However, if the stability of the CSD simulation is problematic at very small azimuthal increments, or other reasons to maintain these disparate time increments exist, then the larger CSD increments of azimuthal motion require interpolation at each of the smaller CFD time steps to obtain the requisite blade deflections. The accuracy of the interpolation can be evaluated using the time dependent form of the work equation, eqn. 13, for each quantity of interest in a manner similar to the spatial interpolations.

Interpolation Methods

The computational aeroelastician must develop consistent methods of data exchange across the disparate meshes required by the aerodynamic and

structural dynamics models. Herein the one- and two-dimensional methods for lifting-line and lifting-surface representations of the rotor blade evaluated in this study are presented. Additional methods of interpolation are discussed and evaluated for non-rotorcraft methods in Refs. [16] - [21], to name a few.

1-D Methods

One-dimensional interpolation methods that have been evaluated include the proximal (nearest-neighbor) interpolation, linear interpolation and cubic spline. Two forms of cubic splines are explored, natural and Hermite cubic splines. These methods were chosen to provide a range of interpolations from the simple point sampling to methods with C^2 continuity.

Proximal interpolation is also known as nearest-neighbor interpolation and point sampling. For an input location x within the bounds of a one-dimensional array of data, the nearest point in the array is located, and the value of the function at the point is assigned to the input location, yielding a piecewise-constant interpolation. Consider an input location, x , then the nearest-neighbor search of a one dimensional array of length N yields an $f(x_j)$ such that $\{x_j : 1 \leq j \leq N \text{ and } \exists x_j : \min(x - x_i) \text{ for all } i = 1, N\}$. This is the least expensive of all of the interpolation methods with no additional array storage beyond the original database and an operation count of $\mathcal{O}(N + 3)$, where N is the array cardinality, assuming that all of the array nodes are examined.

Linear interpolation is an approximation based on the definition of a local linear polynomial about the input location $\{x : x_i \leq x \leq x_{i+1}\}$ where

$$f = f(x_i) + (x - x_i) \frac{(f(x_{i+1}) - f(x_i))}{(x_{i+1} - x_i)} \quad (14)$$

This yields a function that is C^0 continuous. In one dimension, the approximate cost of this function is $\mathcal{O}(N + 6)$, and it does not require additional array storage beyond the database array.

Cubic Splines comprise a popular piecewise polynomial interpolation technique that minimizes the errors compared to a polynomial interpolation, avoiding overshoots (Runge's phenomenon) that may appear with higher-order polynomial interpolation. The cubic spline, $S(x)$, is constructed for $n+1$ data points to create n piecewise cubic polynomials so that

$$S(x) = \begin{cases} S_0(x) & x \in (x_0, x_1) \\ S_1(x) & x \in (x_1, x_2) \\ \dots & \\ S_{N-1}(x) & x \in (x_{N-1}, x_N) \end{cases} \quad (15)$$

with the additional requirements at the database array

$$\begin{aligned} S(x_i) &= f(x_i) & i &= 1, N \\ S_{i-1}(x_i) &= S_i(x_i) & i &= 1, N-1 \\ S'_{i-1}(x_i) &= S'_i(x_i) & i &= 1, N-1 \\ S''_{i-1}(x_i) &= S''_i(x_i) & i &= 1, N-1 \end{aligned} \quad (16)$$

to ensure C^0 to C^2 continuity. The cost of this function is approximately three times the cost of the linear interpolation method.

Hermite Cubic Splines are a form of cubic splines that are third-degree and cast the spline polynomials in Hermite form. Hermite form requires that each piecewise polynomial basis include two control (end) points and two tangents [22]. The tangents provide a further form of control of the local spline, and in some instances can provide smaller errors in the interpolation. However, the penalty of this method is the cost, which is approximately double the cost of the natural cubic spline.

2-D Methods

For lifting-surface applications, the 1-D interpolation methods above can be extended to include 2 dimensions. However, based on the fixed-wing studies discussed previously, it is clear that to provide consistent equivalence in properties across the fluid/structure interface, advanced methods are required. Two methods are demonstrated within the framework of this work, multiquadric-biharmonics (MQ) and thin plate splines (TPS). These were chosen due to the ease by which they can be utilized in existing methods without code reformulation.

In prior studies [18, 19], these methods were shown to be accurate and robust compared to similar interpolation techniques. MQ requires that at least two of the three Cartesian coordinate directions for the surface be single-valued. While MQ works very accurately for small extrapolation areas, it can distort the overall function when large extrapolation areas are required. For disparate grid scales (such as the rotor blade radius compared with the chord), these methods are more accurate when they are scaled to $(x, y, z) \in [0, 1]$.

Multiquadric-biharmonic (MQ) method is an interpolation technique that represents an irregular surface, defined in terms of the coordinates of a set of N points, in terms of a set of quadratic basis functions. Kansa [23] has shown that the method's conditioning, accuracy, and general numerical performance are improved by (1) permitting the shape parameter, r , to vary among the basis functions; (2) scaling and/or rotating the independent variables so that $(x, y, z) \in [0, 1]$; and (3) applying it in overlapping subdomains

to reduce matrix inversion costs. The multiquadric method is the summation of quadric surface equations with unknown coefficients to represent irregular surfaces. This method was originally developed by Hardy [24] to construct a function $H(x)$ given its values at a set of N discrete nodal values $H_i = H(x_i)$ at nodes $\mathbf{x} = \mathbf{x}_i$, for $i = 1, 2, \dots, N$. The interpolation equation is written as

$$H(\mathbf{x}) = \sum_{i=1}^N \gamma_i ((\mathbf{x} - \mathbf{x}_i)^2 + r^2)^{0.5} \quad (17)$$

where the coefficients γ_i are to be found. In order to find the values of the coefficients γ_i one simply applies this equation to each of the N points yielding

$$H(\mathbf{x}) = \sum_{j=1}^N \gamma_j ((\mathbf{x}_i - \mathbf{x}_j)^2 + r^2)^{0.5} \quad (18)$$

Per Kansa [23], the shape parameter, r , is computed as

$$r_j^2 = r_{\min}^2 \left(\frac{r_{\max}^2}{r_{\min}^2} \right)^{\frac{j-1}{N-1}} \quad (19)$$

where the minimum and maximum values of r are user defined.

Thin-plate splines (or surface splines) provide a means to characterize an irregular surface by using functions that minimize an energy functional. This methodology is very similar to the MQ method, but the primary difference in these two methods is the choice of the basis functions. Here, the problem is approached from an engineering representation of the surface. That is, for a one-dimensional (1-D) problem, elementary cubic splines can be interpreted as equilibrium positions of a beam undergoing bending deformation. For a 2-D problem (such as a surface), these splines can be determined from the minimization of the bending energy (thus defining the equilibrium position) of a thin plate. Since these types of splines are invariant with rotation and translation, they are very powerful tools for the interpolation of moving or flexible surfaces, and act in a manner similar to finite-element basis functions.

The methodology applied here was verified mathematically by Duchon [25]. The bending energy for a thin plate extended to multi-dimensional domains is

$$\Phi = \int_{\mathcal{R}} |D^m v|^2 d\mathcal{R} \quad (20)$$

where $m > l/2$ when discrete values are used (as is the case here). this functional is very easy to solve. The basis function can be written as

$$H(\mathbf{x}) = \beta_0 + \beta_x x + \beta_y y + \beta_z z_i + \sum_{j=1}^N \gamma_j (\mathbf{x}_i - \mathbf{x}_j)^2 \log |\mathbf{x}_i - \mathbf{x}_j| \quad (21)$$

The coefficients γ_i , for $i \in [1, N]$, and $\beta_0, \beta_x, \beta_y, \beta_z$ are determined by solution of the minimization problem with the additional constraints that

$$\sum_{i=1}^N \gamma_i = \sum_{i=1}^N \gamma_i x_i = \sum_{i=1}^N \gamma_i y_i = \sum_{i=1}^N \gamma_i z_i = 0 \quad (22)$$

These can be expressed in matrix form as $\{\mathbf{H}\} = [\mathbf{B}]\{\boldsymbol{\gamma}\} + [\mathbf{R}]\{\boldsymbol{\beta}\}$ and $[\mathbf{R}]^T\{\boldsymbol{\gamma}\} = 0$.

Results

For all computations, the errors presented are relative errors that have been computed via the expression

$$\epsilon = \frac{(f_{exact} - f_{predicted})}{f_{exact}} \times 100 \quad (23)$$

and are presented as percentages. To ensure that the interpolation methods are performing correctly, the data have been interpolated across identical grids (CFD grid is identical to the CSD grid) and the work error has been verified to be zero (within the computational accuracy of the machine).

1–D (Radial) Blade Modeling

The first evaluation of the equivalence of spatial quantities is the interpolation across the aerodynamic and structural meshes. If a structural beam model is assumed, the aerodynamic loads and moments can be integrated and transferred along a radial line from blade root to tip. This radial line is typically chosen to be the quarter-chord or elastic axis, as denoted in Fig. 2, for both structured and unstructured CFD grids. The loads on the beam linearly increased from the root to the tip, as did the blade deflection. This is followed by an evaluation of actual CFD-CSD simulations.

Spatial Interpolation: Load–Deflection Data

This test sequence was designed to evaluate the errors associated with the interpolation methodology. Thus, the work computed from the CFD grid is assumed to be the exact work, and will form the baseline comparative value. Four popular interpolation methods,

described previously, were evaluated, along with variations in the nodal locations to determine the constitutive error sources and lead to a best-practices recommendation.

The set of nodal locations that comprised the CSD airstations (r_{csd}) for this study was based on constant spacing in addition to a grid that utilized clustered nodes at the root and tip where the aerodynamic values may rapidly change. The algorithm for the constant spacing is based on

$$r_{csd_i} = r_{cfd_{min}} + (r_{cfd_{max}} - r_{cfd_{min}}) \frac{(i-1)}{(N_{csd}-1)} \quad (24)$$

where N_{csd} is the total number of CSD airstation locations. Care was taken to ensure that this problem remained one of interpolation, without extrapolation. The sets of constant spaced airstations chosen for study include $N_{csd} \in [i : 10 \leq 10 * i \leq 500]$ and assuming $N_{cfd} \in [j : 81 \leq 80 * j_{math} + 1 \leq 401]$ to determine the characteristics of the work conservation for a wide range of fidelity of CFD grids and airstation combinations.

The results of interpolations using these parameters is illustrated in Fig. 3 via the average work error. Using a simple comparison of the summed forces, the interpolations appear to be very accurate, as the relative errors decrease from the $\mathcal{O}(10^{-5})$ to $\mathcal{O}(10^{-7})$ as the number of radial stations increases. The relative errors associated with the work are typically 2 to 3 orders of magnitude higher than the relative force errors. The average work error appears to indicate that all of the interpolation methods are comparable, implying that the best (most efficient and accurate) interpolation method would be the proximal or linear interpolations, given the mean cost of each method is 1.0, 0.4726, 0.1664, 0.1481 for the Hermite cubic, cubic, linear, proximal methods, respectively. However, further insight into the accuracy of the methods can be obtained from Fig. 4, which illustrates the behavior of the interpolation methods for two of the N_{cfd} cases. The proximal interpolation method clearly does not provide the accuracy implied in the average results, as there is significant scatter associated with the method, with no clear basis to assess when the method will provide minimal errors.

For the remainder of interpolation methods, the relative work error indicates that the while $N_{csd} < N_{cfd}$, the error decreases as N_{csd} approaches N_{cfd} until it reaches 1 – 3 optimal grid distributions, followed by error growth that smoothly increases until it reaches a limiting value when $N_{csd} \gg N_{cfd}$. The optimal equally spaced CSD grid distribution is determined when the distance between the CSD airstations correlates with the average distance between CFD node and midpoint, that is $\Delta r_{csd} \approx 0.5 \Delta r_{cfd_{max}}$

and has the most locations that coincide closely with the midpoints of the CFD nodes. As the number of CFD nodes are increased, the number of CSD nodes needed to achieve minimal error is seen to scale approximately linearly, but not usually with a slope of 1 as the minimal error depends on the CFD grid distribution. Further, the magnitude of the minimal error at the optimal location(s) decreases approximately two orders of magnitude as the CFD fidelity increases initially, although a point of diminishing return is rapidly encountered, as shown in Fig. 5. Similar trends are seen with CSD grid distributions that are refined near the tip and root.

Consider next these interpolations when applied not to an instantaneous theoretical application, as was just described, but as one interpolation step in the loose coupling process described in Fig. 1. These computations were accomplished in the radial direction for 1° azimuthal increments and were not interpolated in the azimuthal direction. The relative errors due to both the work and loads are shown in Fig. 6. As noted previously, the use of loads (forces and moments) as a measure of accuracy alone leads to the conclusion that the interpolations are more accurate than they are within the aeroelastic application for which they are used. In contrast to the prior theoretical beam example, the loads errors are only a factor of 2 – 3 rather than 2 – 3 orders of magnitude lower than their work error counterparts. The example provided in Fig. 6, is that of the 81 station CFD grid. From the prior study, it was noted that the minimal error occurred with 50 equally spaced CSD airstations, which is also seen to be true for the full rotor interpolation as well. The cubic spline performs best of the interpolation methods, and it is noteworthy that larger differences using work (rather than forces) are now observed between the Hermite cubic spline implementation compared with the standard cubic spline.

The impact of these interpolations on the rotor are illustrated with Figs. 7 and 8. The differences in the linear and spline interpolation results are not discernible visually, so one figure is used to illustrate these group results. The proximal interpolation is characterized by discontinuities in the deflection and force/moment interpolations, as illustrated in Fig. 7b and 8b. These discontinuities are observed for all combinations of CFD and CSD node selections and occur for interpolations in deflections, forces and pitching moments. While not readily apparent, the differences in the CFD (a) and non-proximal interpolations (c) are in areas with small radial expanses and/or with rapid changes, such as the tip region of the pitching moment.

Temporal Interpolation: Motion Data

In the prior studies, all interpolations were made at identical azimuthal locations for the rotor. However, unlike the prior spatial examples where data can be mined at any set of airstations without affecting the overall cost or accuracy of the CSD simulation (when using finite-elements), temporal location changes will impact the CSD simulation time. Depending on the flight conditions of the rotor, typically the CSD simulation can be run at 5° azimuth increments to obtain accurate results, while the CFD code must be run at $< 1^\circ$ azimuthal increments. As noted previously, running the CSD simulation at the same azimuth increment as the CFD code will result in no work errors due to temporal interpolation (since there is none). However, this can add significant costs to loosely-coupled simulations, and it of interest in tightly-coupled simulations as freezing motion during small azimuthal increments is a way to increase the efficiency of the CFD–CSD simulations.

The results of the temporal interpolation are very similar to those of the spatial interpolation. Figure 9 illustrates the results for 5° azimuth interpolation. It is obvious that the discontinuities that resulted from the spatial interpolations are again observed for temporal integrations. The influence of interpolation using the most accurate methods are depicted in Fig. 9 a and c, in conjunction with Fig. 10. For this case, the interpolation methods begin to lose accuracy at 15° azimuth interpolation for the smaller features of the motion. The trends in the errors are comparable to the spatial interpolations previously discussed.

CFD–CSD Rotor Simulations

The initial beam simulations provide understanding of behavior of the interpolation, and overall the study indicates that for a single interpolation, the techniques evaluated result in less than 1% error in virtual work when transferring data between the CFD and CSD methods. However, for CFD–CSD rotor computations, it is necessary to understand the consequences of the interpolation errors on the simulation. Thus, the next step is to apply the results of the prior studies to a CFD–CSD rotor problem of interest. The CSD method utilized for these simulations is DYMORE [1], using a C^0 finite element beam model.

For this evaluation, the impact of the CSD airstation locations for a given interpolation method is studied. It was observed that the interpolation errors were minimized for the 81 radial station CFD grid at about 50 airstations, with all methods except the proximal method yielding approximately comparable interpolation accuracy. Fig. 11, which illustrates the cubic spline method clearly indicates that

the small interpolation errors can have a significant impact on the CFD–CSD simulation. The 81-station result at the 77% radial station provides the result obtained without spatial or temporal interpolation. The 41-station result is closest to the minimal error distribution observed for the spatial interpolation, while the 21-station and 61-station show that the predicted deflections are not as accurate, and that work errors are increasing, as expected. Similar trends are observed for normal force and pitching moment for these simulations, and these results are comparable to the observations of Farhat [16] in fixed-wing applications. Other important results that are extracted from a CFD–CSD simulation are the controls needed to achieve the trimmed solution. For these results, a given thrust coefficient and zero pitching/rolling hub moments were utilized as the basis for trim. The 41-station and 61-station results remained, respectively, within 10% and 15% of the predicted controls (collective and cyclics). The 21-station results were 40% to 50% in error with respect to the non-interpolation results. This is comparable to differences of 1° (41-stations) to 5° (21-stations) in collective. These results were found to be repeatable for another test case evaluated using the same parameters. For high thrust and maneuvering cases on the edge of the flight envelope that are of particular interest to the research community, the over prediction in the collective, which is needed to achieve trim, could result in failure of the CFD–CSD methodology.

Unstructured CFD Methods

The question of conservation during the data exchange between a structured CFD and the CSD methodologies can be avoided if the airstations are chosen to lie at the radial CFD grid locations. However, as illustrated in Fig. 2c, unstructured CFD methods are constrained to use interpolation when a surface mesh of triangular faces is employed. Thus, the surface loads must be converted into one-dimensional lifting-line format so that it may be used by the CSD code. To accomplish this, the CFD rotor surface is first divided into panels that mimic structured grid radial stations extending from leading edge to trailing edge, where the center of each panel corresponds to an airstation on the lifting-line model.

There are two methods to obtain the forces and moments for these airstations. The first is to slice the blade along a radial station that intersects the point and the blade surface from leading to trailing edges, resulting in forces and moments per unit length. These are then integrated over the panel area and evaluated similarly to the structured CFD method. A second approach is to sum integrated forces from each CFD surface cell that lie within the

panel are to define the total forces and moments acting on the panel. This has the potential to capture changes in the physics over small areas (for example, loads from a micro flap or piezoelectric device that is smaller than the extent of the defined panel) without *a priori* knowledge of the loading.

When implementing the second approach, it is necessary to recognize that an unstructured cell may not necessarily be contained within a single airstation panel. If the load is assumed to be constant over the CFD cell, then this issue can be addressed by computing the percent of the cell area present in each panel, yielding an exact representation of the loading, or a proximal (nearest-neighbor) assumption can be made. The impact of the proximal assumption can be seen in Fig. 12, which compares the resulting airstation loading during the CFD–CSD coupling process. The proximal method results in a piecewise airloads profile over the azimuth, along with a significant loss of accuracy, indicating a loss in virtual work, as per Farhat’s analysis [16] and that observed herein for the structured grid.

While the linear interpolation and spline interpolations yielded very similar results for the interpolation of the blade motion, their application in the unstructured methodology provides results that are not as comparable, as observed in Fig. 13. The cubic spline provides a much smoother deflection, similar to that for the unstructured method, while a simple linear interpolation to the unstructured nodes includes what appear to nonphysical oscillations.

2D Spatial Conservation

While the primary focus of CFD–CSD coupling to date has focused on the assumption that a beam model can correctly represent the structure of the rotor, research into advanced concepts such as aeroelastic tailoring of the rotor blade via piezoelectric controls will require that the rotor blade be structurally modeled as a plate or shell. Thus, the loads-deflection interchange will require that two-dimensional interpolation be applied. For this application, the researcher may once again utilize the CFD grid to set up airstations where the structural model is to be queried for deflection information. If the CSD methodology can extract this information directly from the finite elements at airstations that are centered within each CFD node, then conservation between the grids is assured. If it is not possible, then again interpolation is necessary, now with two-dimensional methods.

Two-dimensional interpolation methods for fixed-wing CFD–CSD coupling are widely published, as noted previously. Therefore, the application of two of these interpolation methods will be directly evalu-

ated for a typical rotor blade in level flight. In order to include illustrations that are visually significant, figures will be restricted to the blade tip region. The original CFD tip grid includes 41 radial stations with 56 chord stations, shown with the force distribution in Fig. 14. The CSD surface is composed of equidistant 11 and 21 radial airstations, in combination with 21, 41 and 61 chord airstations.

The magnitude of the errors in two-dimensional applications is much higher than its one-dimensional counterpart, as shown in Fig. 15. Increasing the number of stations in the radial direction yields a trend of diminishing return similar to that observed previously for one-dimensional applications (Fig. 6). Increasing the number of airstations along the chord improves the interpolation as well, although the cost of the interpolation is prohibitive to increasing the number of points without the addition of computational partitioning, as noted in the method description. The thin plate spline (TPS) method appears to be more sensitive to the number of chord airstations compared with the MQ method. As the number of chord airstations is increased, the methods yield comparable accuracy in the interpolations.

Further analysis, including CFD-CSD coupling is planned with both unstructured and structured methods in the near future.

Conclusion

It has been demonstrated that the choice of interpolation method and selection of airstations for the exchange of data across the fluid/structure interface can impact the ability of CFD-CSD coupling methods to predict accurate loads. It is recommended for lifting-line (beam) CSD representations of rotors that

- Airstations are located along the reference axis at the midpoint between each CFD radial node to avoid interpolation in structured grids. This will not require modification of or additional cost in finite-element models that allow airstation queries of the consistent basis function.
- When interpolations are necessary, airstations are located so that the minimum error is obtained after interpolation. This requires airstations to be located near the CFD nodes or midpoints, and they should be tailored for each new CFD grid. The airstation locations can be scaled linearly if the CFD grid distribution remains the same during grid refinement.
- The interpolation method should be chosen to be C^0 or higher. For this work, the CSD finite element model enforced C^0 continuity. Proximal methods should be avoided.

- Use of total forces and moments as a measure of accuracy are not as informative as the equivalence of work across the fluid/structure interface.
- Unstructured CFD codes must utilize some form of interpolation, and they also appear to be more sensitive to the interpolation methods. They may require higher levels of continuity (C^n) to be as accurate as their structured CFD counterparts.

As researchers investigate advanced aeroelastic tailoring of rotor blades, lifting-surface structural representations will be necessary.

- Surface representations are more sensitive to interpolations, and it is more difficult to preserve work across the fluid/structure interface.
- Interpolation techniques that preserve work across the fluid/structure interface has been a topic of study within the fixed-wing community and their applicability to rotor blades have been demonstrated.
- Additional research in this area is planned in the near future.

Acknowledgments

First and foremost, the author is indebted to Prof. Olivier Bauchau at Georgia Tech, not only for this paper, but throughout the years for the many technical conversations on structural dynamics and CFD-CSD coupling. While he provided many insightful comments for this work, any mistakes herein are the author's own. The author would like to thank the Non-linear Computational Aeroelasticity Lab (NCAL) at Georgia Tech for their contributions to this work, including Jennifer Abras, Yann Vonderscher, and Eric Lynch, specifically, who all contributed data from their respective research. The author would like to thank Nic Reveles in particular for his unstinting efforts that contributed to this study.

Computational support for the CFD simulations was provided through the DoD High Performance Computing Centers at MHPCC, ERDC and NAVO through an HPC grant from the US Army. Dr. Roger Strawn is the S/AAA of this grant. The computer resources of the Department of Defense Major Shared Resource Centers (MSRC) are gratefully acknowledged.

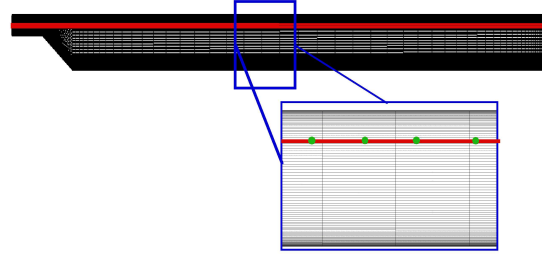
References

- [1] Bauchau, O.A., Bottasso, C.L., and Nikishkov, Y.G., "Modeling Rotorcraft Dynamics with Fi-

- nite Element Multibody Procedures.” *Mathematical and Computer Modeling*, Vol. 33, 2001, pp. 1113–1137.
- [2] Abras, J. N., Smith, M. J., and Bauchau, O. A., “Rotor Airload Predictions Using Coupled Finite Element and Free Wake Methods.” Presented at the American Helicopter Society 62nd Annual Forum, Phoenix, AZ, May 9–11, 2006.
- [3] Saberi, H., Khoshlahjeh, M., Ormiston, R. A. and Rutkowski, M. J., “Overview of RCAS and application to advanced rotorcraft problems.” AHS International 4th Decennial Specialists’ Conference on Aeromechanics, Jan 21-23 2004, San Francisco, CA, 2004, p 741-781.
- [4] Johnson, W., “Rotorcraft Dynamics Models for a Comprehensive Analysis.” American Helicopter Society 54th Annual Forum, Washington, D.C., May, 20–22 1998.
- [5] Bir, G., and Chopra, I., “Development of UMARC (University of Maryland Advanced Rotorcraft Code).” American Helicopter Society 46th Annual Forum, Washington DC, May 1990.
- [6] Beniot, B., Dequin, A., Kampa, K., Grunhagen, W., Basset, P., and Gimonet, B., “HOST, a General Helicopter Simulation Tool for Germany and France.” American Helicopter Society 56th Annual Forum, Virginia Beach, Virginia, May, 2–4 2000.
- [7] Kunz, D. L., “Comprehensive Rotorcraft Analysis: Past, Present and Future.” 46th AIAA/ASME/ASCE/AHS/ASC Structures, Structural Dynamics and Materials Conference, Austin, TX, April 18–21 2005.
- [8] Datta, A., Nixon, M., and Chopra, I., “Review of Rotor Loads Prediction with the Emergence of Rotorcraft CFD.” Presented at the 31st European Rotorcraft Forum, Florence, Italy, Sept. 13–15, 2005.
- [9] Smith, M. J., *A Fourth-Order Euler/Navier-Stokes Prediction Method for the Aerodynamics and Aerolasticity of Hovering Rotor Blades*. PhD Dissertation, Georgia Institute of Technology, 1994.
- [10] Bauchau, O. A. and Ahmad, J. U., “Advanced CFD and CSD Methods for Multidisciplinary Applications in Rotorcraft Problems,” AIAA-1996-4151, 6th NASA and ISSMO Symposium on Multidisciplinary Analysis and Optimization, Bellevue, WA, Sept. 4–6, 1996.
- [11] Beaumier, P., Costes, M., Rodriguez, B., Pointot, M., Cantaloube, B., “Weak and Strong Coupling Between the elsA CFD Solver and the Host Helicopter Comprehensive Code.” Presented at the 31st European Rotorcraft Forum, Florence, Italy, Sept. 13–15, 2005.
- [12] Shelton, A., Braman, K., Smith, M. J. and Menon, S., “Improved Turbulence Modeling for Rotorcraft, American Helicopter Society 62nd Annual Forum, Phoenix, AZ, May 9–11, 2006.
- [13] Bhagwat, M., Ormiston, R., Hossein, S., and Xin, H., “Application of CFD/CSD Coupling for Analysis of Rotorcraft Airloads and Blade Loads in Maneuvering Flight,” American Helicopter Society 63rd Annual Forum, Virginia Beach, VA, May 1–3, 2007.
- [14] Abras, J. and Smith, M. J., “Rotorcraft Simulations Using Unstructured CFD-CSD Coupling.” AHS Specialists Meeting, San Francisco, CA, January 2008.
- [15] Ananthan, S., and Baeder, J., “Prediction and Validation of Loads on Bearingless Rotors Using a Coupled CFD-CSD Methodology.” American Helicopter Society 64th Annual Forum, Montreal, Canada, April 29–May 1, 2008.
- [16] Farhat, C., and Lesoinne, M., “A Conservative Algorithm for Exchanging Aerodynamic and Elastodynamic Data in Aeroelastic Systems.” AIAA-98-0515, 36th Aerospace Sciences Meeting and Exhibit, Reno, NV, Jan. 12–15, 1998.
- [17] Farhat, C., Lesoinne, M., and LeTallec, P., “Load and motion transfer algorithms for fluid/structure interaction problems with non-matching discrete interfaces: Momentum and energy conservation, optimal discretization and application to aeroelasticity.” *Computer Methods in Applied Mechanics and Engineering*, v 157, n 1-2, Apr 28, 1998, p 95-114.
- [18] Smith, M. J., Hodges, D. H., and Cesnik, C. E. S., “An Evaluation Of Algorithms Suitable For Data Transfer Between Noncontiguous Meshes.” *ASCE Journal of Aerospace Engineering*, Vol 13, No. 2, April 2000, pg. 52-58.
- [19] Smith, M. J., Cesnik, C. E. S., and Hodges, D. H., “An Evaluation Of Computational Algorithms Suitable For Fluid Structure Interactions.” *AIAA Journal of Aircraft*, Vol. 37, No. 2 (Mar-Apr 2000), pg. 282-294.
- [20] Aminpour, M., Pageau, S., and Shin, Y., “Improved Interface Modeling

Technology.” AIAA-2001-1548, 42nd AIAA/ASME/ASC/AHS/AASC Structures, Structural Dynamics, and Materials Conference & Exhibit, Seattle, WA, April 16–19, 2001.

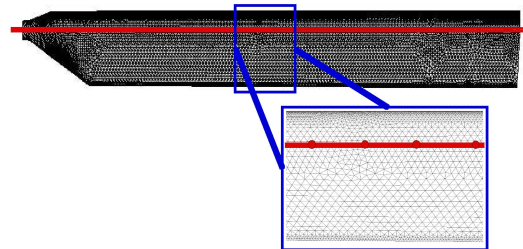
- [21] Ahrem, R., Beckert, A., and Wendland, H., “A Meshless Spatial Coupling Scheme for Large-Scale Fluid-Structure-Interaction Problems.” *CMES - Computer Modeling in Engineering and Sciences*, v 12, n 2, 2006, p 121-136.
- [22] Conte, S. D., and de Boor, C., *Elementary Numerical Analysis: An Algorithmic Approach*. McGraw-Hill Book Company, New York, New York, 1980.
- [23] Kansa, E. J., “Multiquadrics - A Scattered Data Approximation Scheme with Applications to Computational Fluid Dynamics I: Surface Approximations and Partial Derivative Estimates.” *Computers and Mathematics with Applications*, Vol. 19, No. 8/9, 1990, pp. 127 - 145.
- [24] Hardy, Rolland L., “Multiquadric Equations of Topography and Other Irregular Surfaces.” *Journal of Geophysical Research*, Vol. 76, No. 8, March 1971, pp. 1905 - 1915.
- [25] Duchon, Jean, “Fonctions-Spline nergie Invariante par Rotation.” Technical Report R. R. No. 27, Universit de Grenoble, January 1976.



(a) Structured grid with arbitrary CSD airstations



(b) Structured grid with CSD airstations at midpoints of radial grid slices



(c) Unstructured grid

Figure 2: An example of CFD Blade Grids and corresponding CSD airstations.

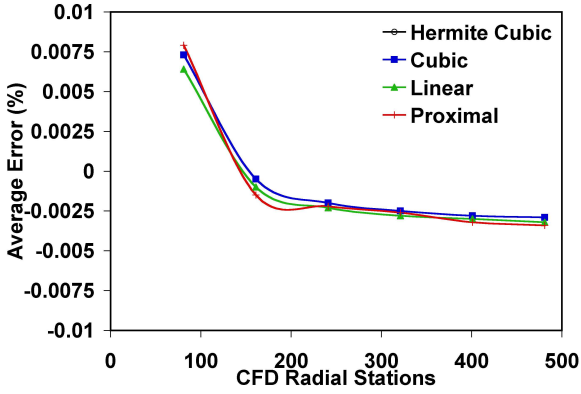


Figure 3: Average one-dimensional (radial) work error due to interpolation.

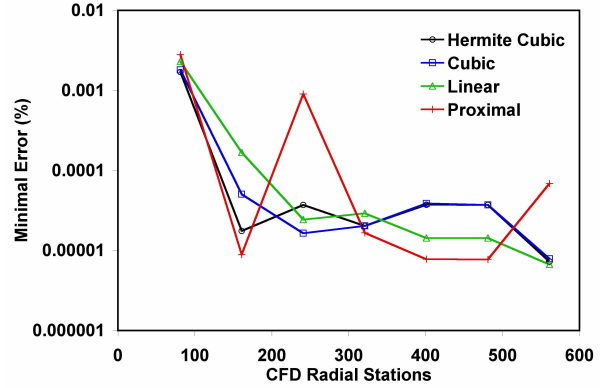
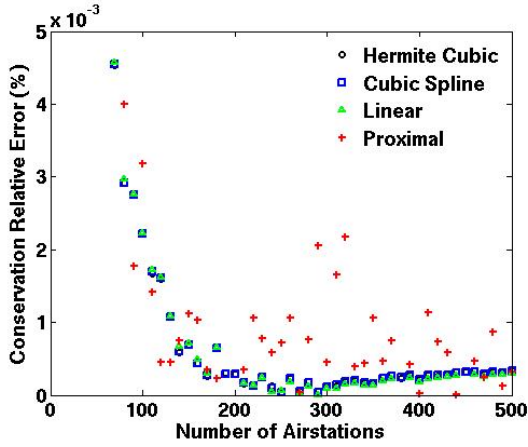
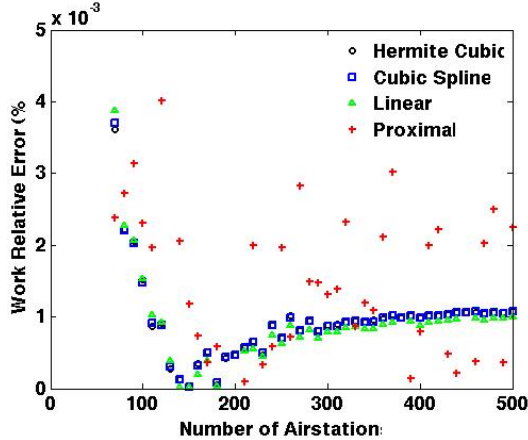


Figure 5: Minimal one-dimensional (radial) work error due to interpolation.



(a) 81 CFD Radial Locations



(b) 241 CFD Radial Locations

Figure 4: Comparison of one-dimensional (radial) work error due to interpolation.

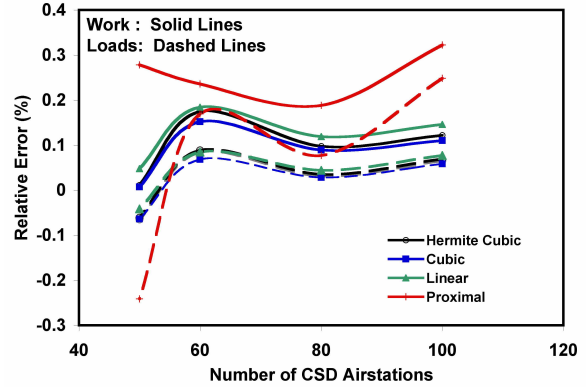
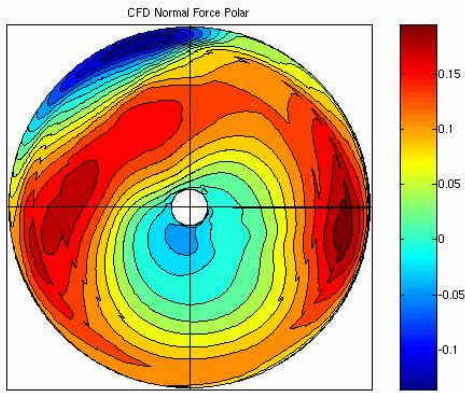
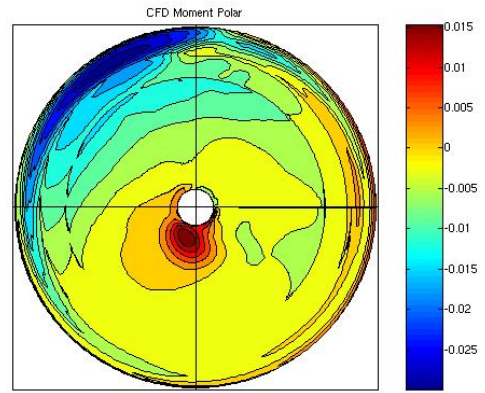


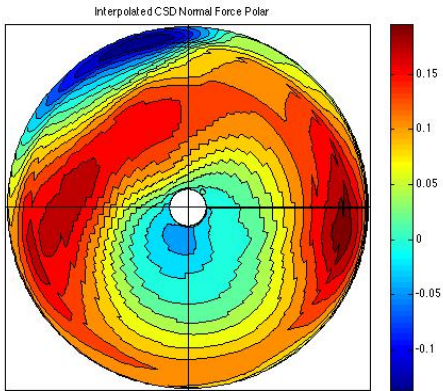
Figure 6: Interpolation errors for a rotor undergoing radial deflections.



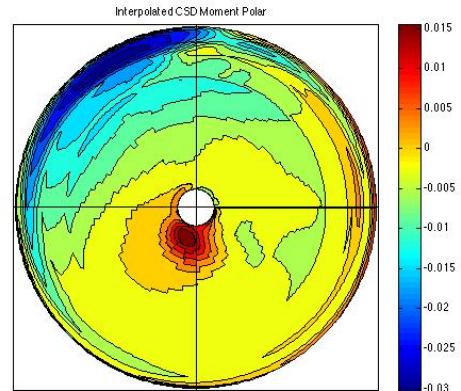
(a) CFD 81 radial station grid



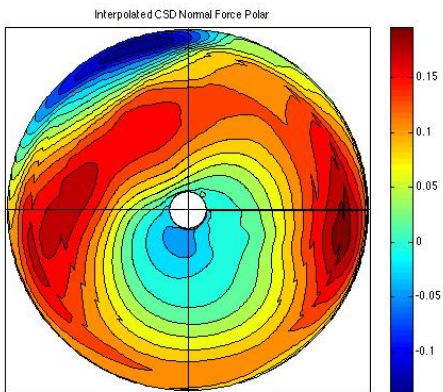
(a) CFD grid



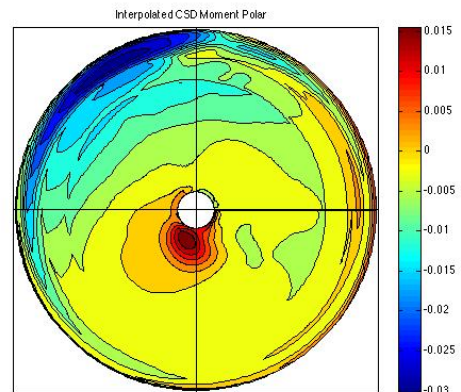
(b) Proximal interpolation



(b) Proximal interpolation



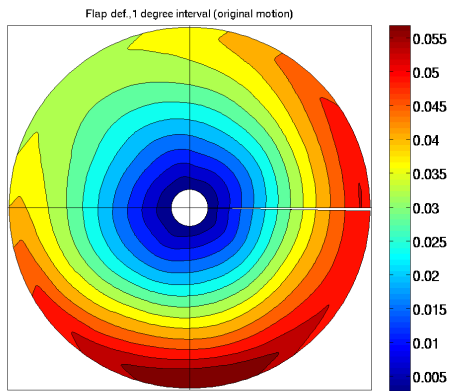
(c) Linear, Cubic Spline, Hermite Spline interpolation



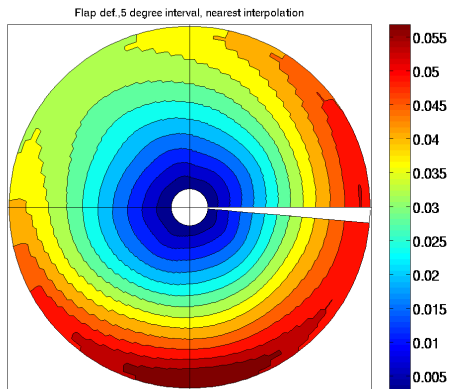
(c) Linear, Cubic Spline, Hermite Spline interpolation

Figure 7: Comparison of one-dimensional (radial) normal force interpolations using 50 equidistant CSD airstations.

Figure 8: Comparison of one-dimensional (radial) pitching moment interpolations using 50 equidistant CSD airstations.



(a) CFD 81 radial station grid, 1° azimuth

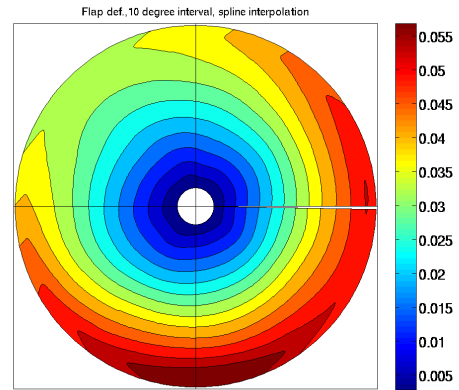


(b) Proximal interpolation

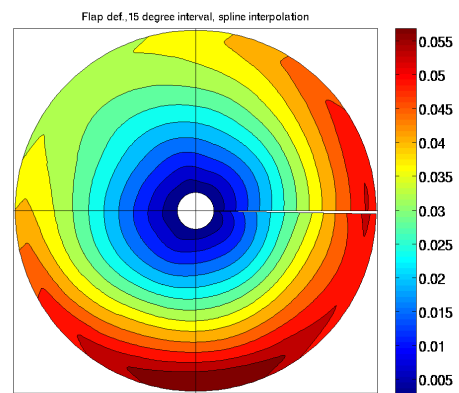


(c) Linear, Cubic Spline, Hermite Spline interpolation

Figure 9: Comparison of normal blade motion using 5° azimuth increments interpolated to 1° azimuth increments.



(a) 10° azimuth increments



(b) 15° azimuth increments

Figure 10: Comparison of normal blade motion at higher azimuth increments interpolated to 1° azimuth increments using spline interpolation.

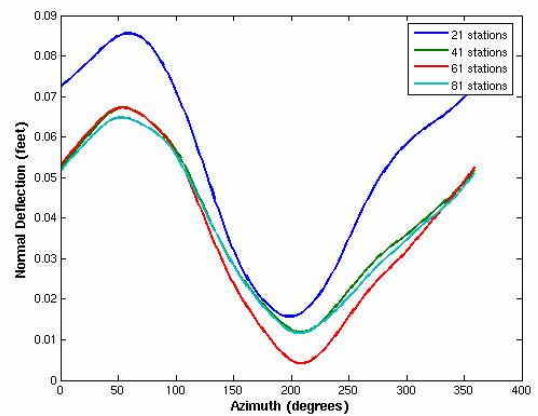


Figure 11: Comparison of normal blade motion using cubic splines after CFD-CSD coupling.

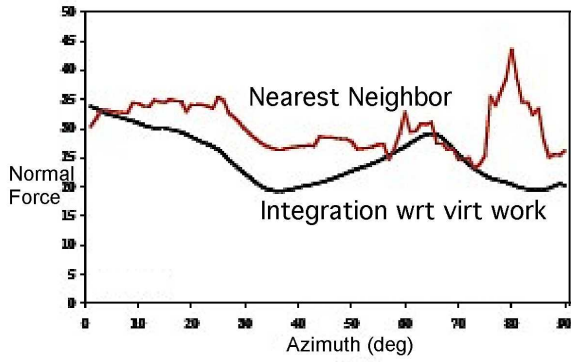


Figure 12: Comparison of airloads with and without overlapping grid surface element division on span station assignments. Figure courtesy of Ref. [14].

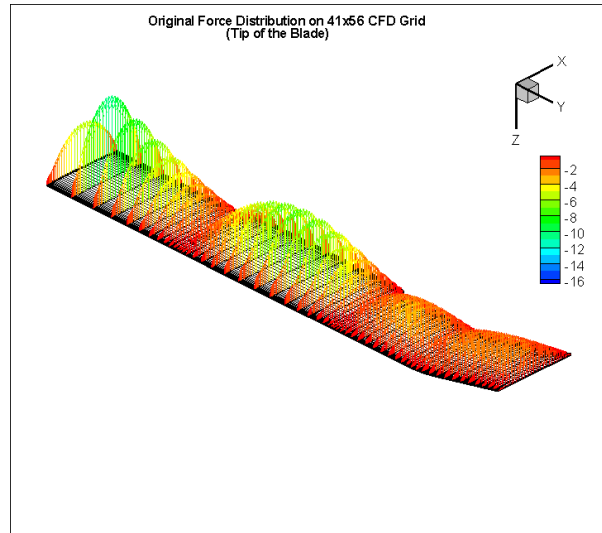


Figure 14: Two-dimensional CFD grid with loads distribution along the tip.

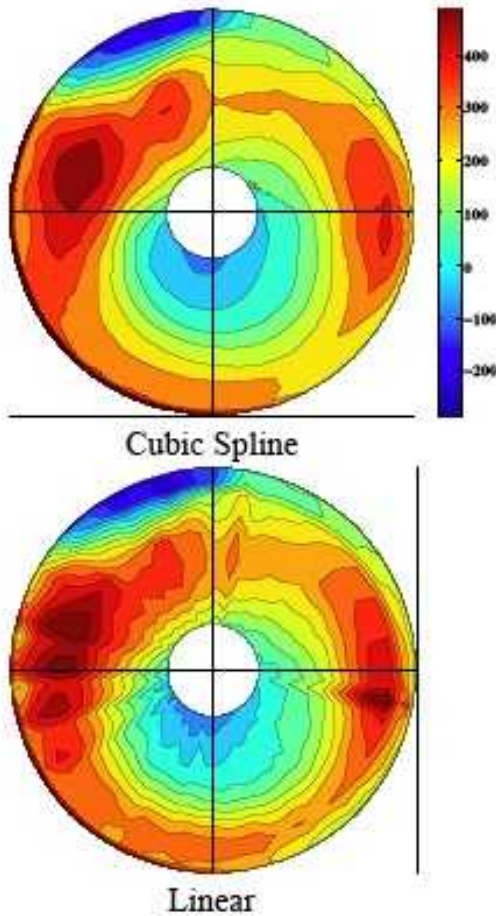


Figure 13: Comparison of interpolation methods applied to grid motion for unstructured lifting-line CFD-CSD coupling. Figure courtesy of Ref. [14].

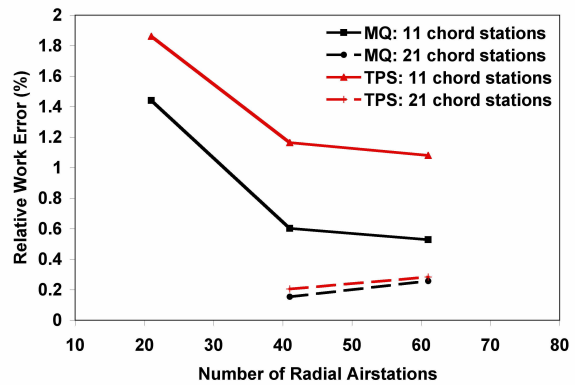


Figure 15: Errors associated with two-dimensional interpolation using multiquadric-biharmonics and thin plate splines.